Available online at www.sciencedirect.com
ScienceDirect
JOURNAL OF IRON AND STEEL RESEARCH, INTERNATIONAL. 2009, 16(3): 55-63

Improvement of Mechanical Properties of Reinforcing Steel Used in the Reinforced Concrete Structures

Oğuzhan Keleştemur[1], M Halidun Kelestemur[2], Servet Yildiz[1]
(1. Department of Construction Education, Faculty of Technical Education, Firat University, Elazig 23119, Turkey;
2. Department of Metallurgical and Materials Engineering, Faculty of Engineering, Firat University, Elazig 23119, Turkey)

Abstract: SAE1010 structural carbon steel, which has a low cost price and wide range of use in the construction industry, has been studied as dual phase (DP) steel subjected to appropriate heat treatment, and its mechanical properties have been investigated under various tempering conditions. Intercritical annealing heat treatment has been applied to the reinforcing steel in order to obtain DP steels with different martensite volume fraction. In addition, these DP steels have been tempered at 200, 300 and 400 ℃ for 45 min and then cooled to the room temperature. Mechanical properties such as tensile strength, yield strength, reduction in cross-sectional area, total elongation, resilience modulus and toughness have been examined. Furthermore, fractographic examination has been done with scanning electron microscope (SEM) as well as metallographic examination of the steels. As a result of this study, it is found that mechanical properties of DP steel have changed according to the hardness and ratio of martensite phase. In addition, tensile strength, yield strength and resilience modulus of the steels have been reduced. In contrast, the total elongation, reduction of the cross-sectional area and toughness have been increased.

Key words: dual-phase steel; reinforcing steel; tempering treatment; mechanical properties

For steels, the desirable mechanical properties are obtained by alloying additions, heat treatment, controlled cold work, and the like. All of these add to the cost of the material and hence to that of the product. Production of steels with improved mechanical properties, but at low additional cost is therefore a matter of practical significance[1]. The most noted achievement of this nature is the high strength low alloy (HSLA) steels[2]. These steels have permitted the designers to achieve appreciable reductions in the weight of cars and the construct large structures at lower cost. However, the HSLA steels at hand have not been able to satisfy the designers needs fully. The methods to develop cheap alternative steels are thus of immediate practical interest[1].

Developed in 1970s dual-phase steels are identified as a class of HSLA steels designated by a composite microstructure constituted by hard martensite particles dispersed in the soft ferrite matrix, where the soft ferrite matrix ensures high formability and the hard martensite provides the strengthening effects[3-6]. In addition to the high tensile strength, dual-phase steels are characterized by continuous yielding behavior, a low yield stress, favorable yield strength to tensile strength ratio (approximate 0.5) and a high level of uniform and total elongation value with a high work hardening coefficient. The combinations of all these properties make them attractive for application as very good quality sheet materials for automotive industries[3-5, 7-9].

The unique combination of mechanical properties has led the researchers to explore the suitability of DP steels for structural and constructional purposes through replacement of pearlite wire, rods and bars[10-12]. But, a carefully conducted review of literature has indicated that reports on improving the mechanical properties of reinforcing steel by dual-phase heat treatment are very limited[1,13,14]. Additionally, a study on effect of tempering heat treatment on the mechanical properties of these steel doesn't exist. The studies performed to determine

Biography: Oğuzhan Keleştemur(1975-), Male, Doctor; **E-mail**: okelestemur@firat.edu.tr; **Revised Date**: December 1, 2008

mechanical properties of dual-phase steel obtained from reinforcing steel have not cleared the subject enough. Therefore, further studies on mechanical properties of DP steel produced from reinforcing steel; especially for various tempering conditions is needed for effective use of these steels in construction industry.

In this study, SAE1010 structural carbon steel, which is the fundamental construction material of construction industry and wide range of product in Turkey, has been studied as dual-phase steel by applying appropriate heat treatment and its mechanical properties have been investigated for various tempering conditions.

1 Experimental Procedure

The rounded bar of SAE1010 steel, which is common construction material in the market and produced in the steel industry of Turkey such as Ereğli Iron and Steel Factory, were selected for the present study as a material to produce dual phase steel. The as-received material was in the form of 12 mm diameter hot rolled bar with a ferrite-pearlite structure. The chemical composition of the steel is given in Table 1 (in mass percent).

The critical heat treatment temperatures of the steel were determined by microscopic examination of heat treated specimens. Starting at 680 ℃, the specimens were heat treated in a neutral salt bath for environmental protection and then quenched in a mixture of ice+water (+1 ℃). The procedure was repeated at 10 ℃ intervals. From the microscopic examinations, 730 ℃ and 840 ℃ were found to be sufficiently close to the A_1 and A_3 (critical temperatures of the iron-carbon equilibrium diagram of steel) temperatures, respectively. However, above 840 ℃ temperatures, it was not possible to transform the austenite to martensite effectively due to the low carbon content of austenite which impaired its hardenability. The specimens were heat treated at 730 ℃ to increase carbon content in austenite phase.

Small specimens of 15 mm in length were cut out from the as-received material for metallographic examinations. Tensile specimens were also machined from the as-received material.

Table 1 Chemical composition of steel %

w(C)	w(Si)	w(Mn)	w(P)	w(S)	w(Fe)
0.176	0.231	0.557	0.011	0.027	Balance

All specimens were heat treated for 20, 40 and 60 min in the intercritical range (730 ℃) and quenched in a mixture of ice+water (+1 ℃). Duration of austenization treatment was varied to obtain different martensite volume fraction. All specimens were tempered at 200, 300 and 400 ℃ for 45 min after quenching and then left to the room conditions. In order to distinguish the specimens subjected to varied heat treatment schedules, they were identified with code numbers, as described in Table 2.

All the heat treatment cycles were carried out in a neutral salt bath whose temperature was controlled at ±1 ℃ for atmospheric environmental protection.

Microstructure of the specimens were observed under light microscope following usual metallographic polishing and etching with 2% natal (98% C_2H_5OH + 2% concentrated HNO_3) solution. Quantitative metallographic techniques were employed to determine volume fraction and grain size of the phases. Grain size and volume fraction of the phase constituents have been determined by the method given in ASTM E112[15].

Vickers microhardness measurements were carried out for both ferrite and martensite phase. A "Leitz" microhardness tester was used under 15 g load for 15 s loading time. The microhardness values were obtained by taking 100 hardness measurements from the center of specimen to the edges.

Tensile tests were conducted using specimens whose configuration is shown in Fig. 1. The specimens were pulled at room temperature in a "Hounsfield" Tensometer tester with a 50 kN loading capacity at crosshead speed of 10 mm/min. Load-elongation change

Table 2 Heat treatment schedules for achieving dual phase microstructure

Specimen Code	Temperature/Duration for austenization treatment	Temperature/Duration for tempering treatment
C	—	—
D20	730 ℃/20 min	—
D22	730 ℃/20 min	200 ℃/45 min
D23	730 ℃/20 min	300 ℃/45 min
D24	730 ℃/20 min	400 ℃/45 min
D40	730 ℃/40 min	—
D42	730 ℃/40 min	200 ℃/45 min
D43	730 ℃/40 min	300 ℃/45 min
D44	730 ℃/40 min	400 ℃/45 min
D60	730 ℃/60 min	—
D62	730 ℃/60 min	200 ℃/45 min
D63	730 ℃/60 min	300 ℃/45 min
D64	730 ℃/60 min	400 ℃/45 min

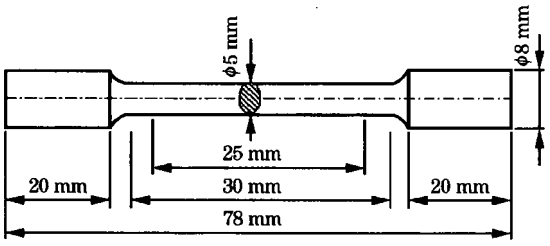

Fig. 1 Configuration of the tensile specimen

were obtained with the aid of x-y plotter which was connected to the device during the tensile test. At least three tensile specimens were tested for each heat treatment condition and average values were calculated.

Fracture surfaces of tensile specimens were observed by using Leo Evo 40VP scanning electron microscope (SEM).

2 Results and Discussion

2.1 Microstructure

Microstructure of the as-received specimen (C) shown in Fig. 2 reveals that the structure consists of uniformly distributed pearlite (dark grains) colonies in an equiaxed ferrite matrix.

Microstructures of DP steels developed by heat treating for 20, 40 and 60 min at 730 ℃ temperature and quenching in a mixture of ice+water are shown in Fig. 3.

It is observed that heat-treating of C specimen directly to the intercritical temperature results in the development of martensite network surrounding ferrite grains (Fig. 3). Such morphological distribution of martensite is commonly termed as ring, chain or continuous network of martensite[16]. Initially, microstructure of the DP specimens has ferrite and pearlite. When annealed in the ($\alpha+\gamma$) region, austenite grains are nucleated at the carbide/ferrite interfaces, which transform to martensite after quenching.

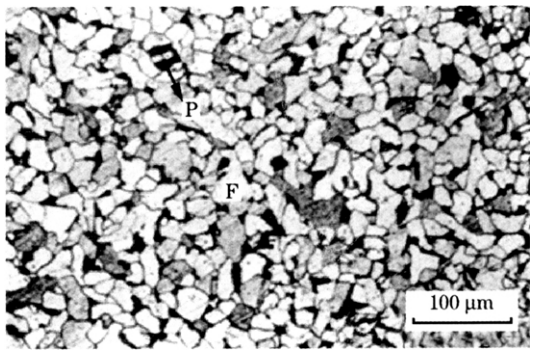

Fig. 2 Ferrite-pearlite structures being processed to produce dual phase steel

The ferrite grains appear unchanged from these observations in the as-received materials. The ferrite phase did not experience any structural change after quenching from the austenite-plus-ferrite region. On the other hand, it is observed on these micrographs that the volume fraction of martensite phase increased with the increase of duration time of austenization. Additionally, pearlite phases have been observed around some of martensite grains on each heat treatment specimen, and pearlite phase surrounding the martensite grains is shown in Fig. 4. However, the amount of pearlite decreased with increasing the duration time of austenization. Similar relationship has also been reported by other researchers[1,12-14,16-24].

The changes on the volume fraction and grain size of the phases are shown in Fig. 5 and Fig. 6.

It is revealed in Fig. 5 that martensite volume fraction increases with increasing of austenization duration. The reason of the increasing of the martensite volume fraction depends on increasing of austenization duration which results increasing the amount of austenite[1,18,25,26].

As seen in Fig. 6, ferrite grain size decreases while martensite grain size increases to some extent with

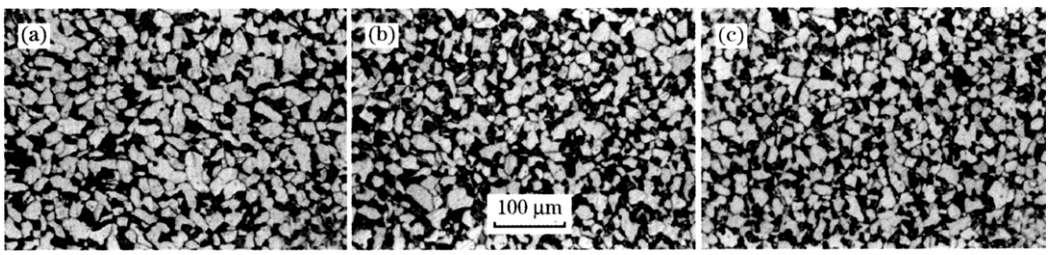

(a) D20; (b) D40; (c) D60

Fig. 3 Microstructures of dual phase steels

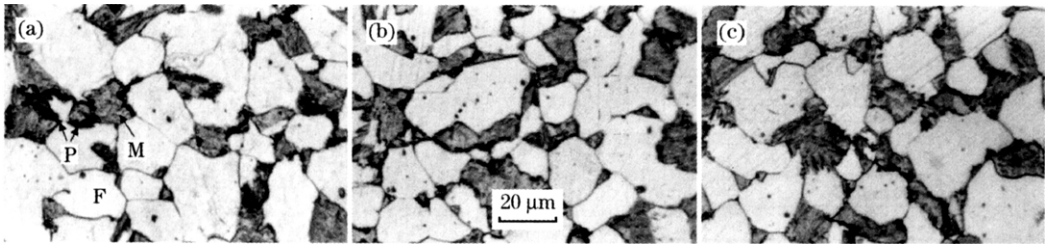

(a) D20; (b) D40; (c) D60

Fig. 4 Microstructure indicating pearlite grains

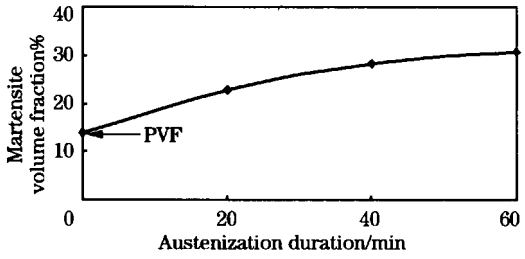

PVF—Pearlite volume fraction

Fig. 5 Variation of the martensite volume fraction depend on austenization duration

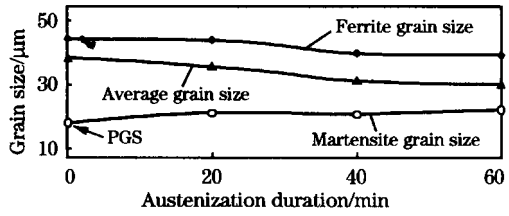

PGS—Pearlite grain size

Fig. 6 Variation grain size of phases with austenization duration

increasing of austenization duration. Because the austenite primarily occurs with the transformation of the pearlite grains. Austenite grains grow while ferrite grains sizes decrease due to progress of the transformation in the ferrite grains. The average grain size of the phases in the microstructure decreases due to decreasing of the ferrite grain size.

2.2 Microhardness

The average microhardness values of the two phases in the specimens are given in Table 3.

As seen in Table 3, the microhardness of the ferrite phases in the dual-phase specimens higher than that of as-received specimen. It can be explained with two ways: first, carbon content in the ferrite phase increases due to austenization treatment and then rapid cooling; second, deformation hardening

Table 3 Microhardness values of the ferrite and martensite phases in specimens

Specimen code	Ferrite microhardness (HV)	Martensite microhardness (HV)
C	157.6	298.6 *
D20	249.9	1 052.3
D22	222.2	867.1
D23	200.9	714.1
D24	191.7	520.1
D40	254.4	926.3
D42	224.3	781.7
D43	204.4	651.8
D44	198.5	504.4
D60	266.7	832.9
D62	226.1	758.5
D63	210.4	621.0
D64	202.6	468.6

* Microhardness of pearlite phase

of the ferrite phase occurs depending on austenite phase transformation to martensite phase during the rapid cooling[17,26]. Deformation ratio of the ferrite phase increases with increasing the martensite ratio. Hence, microhardness of the ferrite phase increases. The relations between the variations of the austenization duration-martensite volume fraction and austenization duration-ferrite microhardness are shown in Fig. 7 due to clarify this situation.

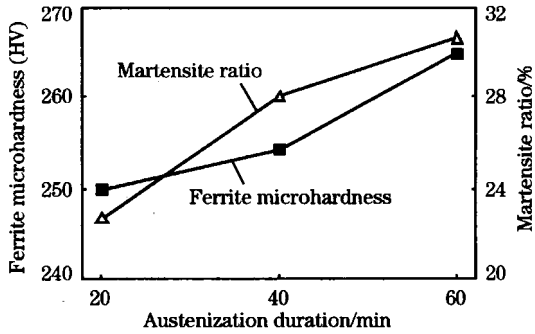

Fig. 7 Variation of martensite ratio and ferrite microhardness with on austenization duration

The volume fraction of martensite and ferrite microhardness increase depending on increasing the austenization duration as can be seen from Fig. 7. The similarity of this increasing is well suited with the explanation.

The hardness of the martensite phase varies depending on the applied heat treatment as can be inferred from Table 3. Very same table also shows that the martensite hardness decreases with increasing the austenization duration, since martensite ratio increases with the austenization duration. Consequently, carbon ratio in the martensite phase decreases and this causes decreasing in the martensite microhardness.

Both ferrite microhardness and martensite microhardness of the tempered specimens decrease with increasing of the tempering temperature. In this situation, decrease in the microhardness of the martensite phase is an expected result. The reason of this decrease can be explained by cementite phase (Fe_3C) precipitation and by decrease in the internal residual stress in the ferrite phase by tempering treatment. Cementite grains in the ferrite phase are shown in Fig. 8.

2.3 Mechanical properties

An example load-elongation curve of the specimens obtained from tensile test is shown in Fig. 9 and other specimens also show similar characteristics.

Fig. 9 shows that serrated flow behavior is not observed on the DP steels, which is one of the characteristics of DP steels during the tensile test. Continuous yielding in these steels can be due to: (1) the transformations of austenite to the hard martensite phase, introducing a high density of mobile dislocations in the adjacent ferrite matrix; and (2) residual stresses from the martensite grains[27,28]. The internal stresses in DP steel decrease depending on increasing of tempering temperature. Hence, the serrated flow in the yield region of the DP steels can be seen on the specimen tempered especially at 400 ℃. These serration flows are also observed in other tensile test specimens.

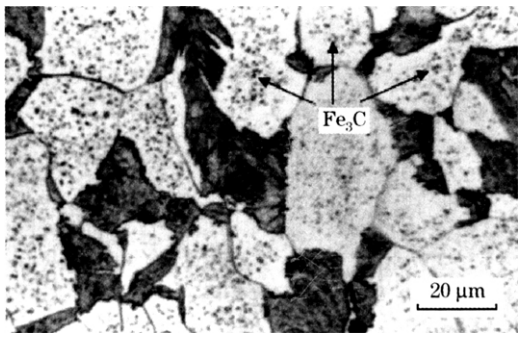

Fig. 8 Optic micrograph indicating cementite grains

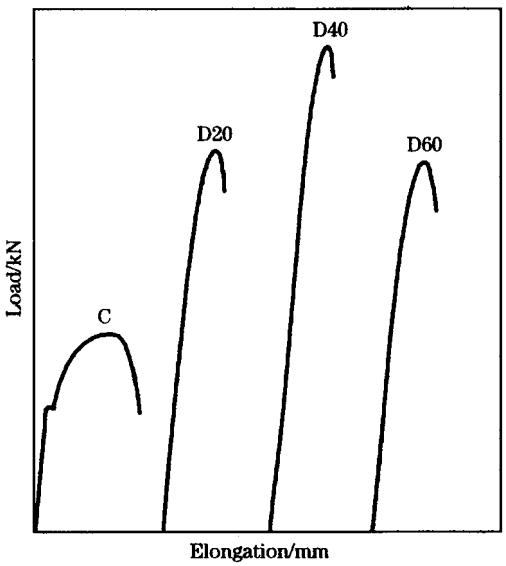

Fig. 9 Load-elongation curves of steels

Average values of the tensile strength (σ_{max}), yield strength ($\sigma_{0.2}$), reduction in cross-sectional area, total elongation, resilience modulus and toughness for the specimens are tabulated in Table 4.

It can be understood from Table 4 that tensile strength, yield strength and resilience modulus of all dual-phase steels are higher than those of as-received specimens. Additionally, elongation and reduction in cross-sectional area values are lower. This can be explained by occurrence of the martensite phase instead of the pearlite phase in the dual-phase steels[1,29,30].

When dual phase induced specimens are compared with each other, it is observed that the tensile strength, yield strength, resilience modulus of the specimens decrease but the total elongation, reduction in cross sectional area and toughness values of them increase depending on increase on the tempering temperature. If these values are considered according to the austenization duration, the results show that the highest values of tensile strength, yield strength and resilience modulus and in a parallel manner the lowest values of the total elongation, reduction in cross sectional area and toughness values are obtained for the 40 minutes of austenization

Table 4 Mechanical properties of specimens

Specimen Code	σ_{max}/ (N · mm^{-2})	$\sigma_{0.2}$/ (N · mm^{-2})	Elongation/ %	Reduction in Area/%	Resilience Modulus/ (N · mm^{-2})	Toughness/ (N · mm^{-2})
C	455	313	30.66	65.21	0.245	118
D20	827	681	8.56	30.79	1.159	65
D22	681	561	11.72	39.72	0.786	73
D23	611	466	15.96	48.68	0.542	86
D24	594	423	17.90	57.20	0.447	91
D40	900	812	7.16	26.74	1.648	61
D42	758	675	9.32	38.81	1.139	67
D43	680	582	11.9	46.08	0.846	75
D44	627	534	13.94	54.04	0.712	81
D60	739	591	11.72	48.77	0.873	78
D62	672	519	13.57	51.26	0.673	80
D63	580	452	15.02	53.73	0.510	81
D64	507	358	19.56	61.27	0.320	85

duration. The lowest martensite volume fraction but the highest microhardness value of it is observed for the 20 minute austenization duration. However, martensite microhardness decreases in spite of increasing the martensite volume fraction for 60-minute austenization duration.

2.4 Fractography

SEM pictures of the fracture surfaces for control and quenched and quenched + tempered specimens are examined. Table 5 summarizes the fracture features of the steels.

General characteristic of the fracture surfaces for all specimens is transgranular. Control specimen shows very high rate necking during the fracture of the specimens, and fracture surfaces show that transgranular and dimple fracture are the main characteristics of it as expected from low carbon steel, Fig. 10 (a), (b), and (c).

The control specimens fail in a ductile mode and there is high rate of plastic flow on specimen fracture surface prior to breakage occurring along the fracture surface, Fig. 10 (a). This flow causes very tiny voids to form within the metal grains as shown in Fig. 10 (b) and (c). As the flow continues these voids grow and coalesce until breakage occurs. SEM micrograph at fairly high magnifications, like shown in Fig. 10 (c), shows remnants of the individual voids exposed on the fracture surface. The fracture is often called micro-void coalescence for obvious reasons.

Table 5 Fracture features of specimens

Specimen	Microstructure	Fractographic appearance	Fracture type
C	Ferrite+pearlite	Transgranular, dimples, high rate necking	Ductile
D40	Ferrite+martensite	Transgranular, facet-like appearance, secondary cracks, cleavage, very low rate necking	Brittle
D42	Ferrite+tempered martensite	Transgranular, low rate facet-like appearance+dimples, very low rate necking	Ductile+brittle
D43	Ferrite+tempered martensite	Transgranular, dimples, high rate necking	Ductile
D44	Ferrite+tempered martensite	Transgranular, dimples, high rate necking	Ductile

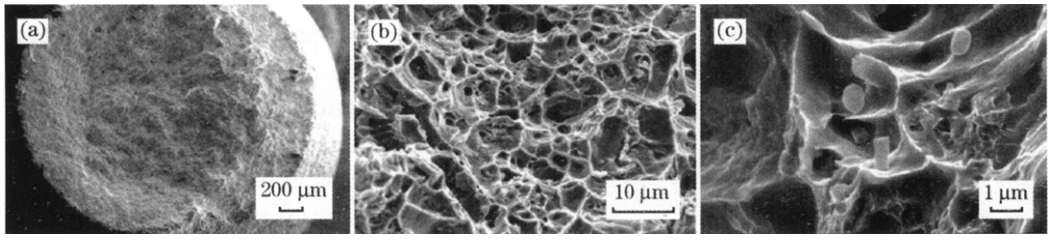

(a) General view; (b) Ductile features; (c) Remnants at voids

Fig. 10 SEM micrograph of C specimen

If the steel contains small foreign particles they will often be the site where the voids first formed and these particles can be seen at the voids on one or the other of the fracture surfaces, Fig. 10 (c). The specimens contained enough small sulfide particles as shown in Fig. 11 on the EDS analysis distributed throughout its volume that many of the voids on the fracture surface reveal the sulfide particles that caused them to nucleate during the plastic flow leading to failure.

The specimen, D40, quenched but not tempered, shows trangranular facet on the fracture surface and proportion of facet is considerably high. Fig. 12 (a) shows that failure has occurred with little to no plastic flow before fracture.

Cleavage fracture surfaces occur and indicate brittle failure. It is well known that cleavage fracture can be defined as rapid propagation of a crack along a particular crystallographic plane, Fig. 12 (b). In this case, although cleavage is a brittle structure and

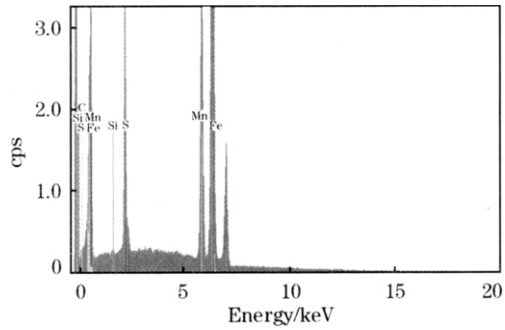

Fig. 11 EDS analysis of C specimen

the crack precedes in a moderate scale plastic flow due to existence of ductile ferrite phases.

All tempered samples show ductile failure characteristics on the fracture surface and high rate necking on the samples. However micro void radius are different for each case, the rate of change of average radius change according to applied tempering temperature parallel to ductility change, Fig. 13 (a), (b) and (c).

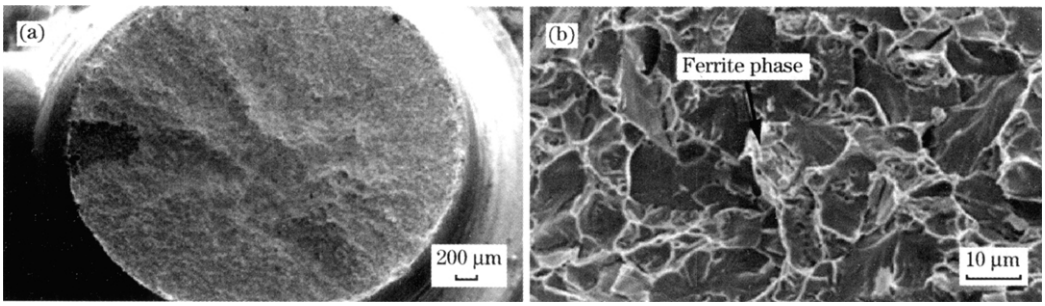

(a) General view; (b) Cleavage features

Fig. 12 SEM micrograph of D40 specimen

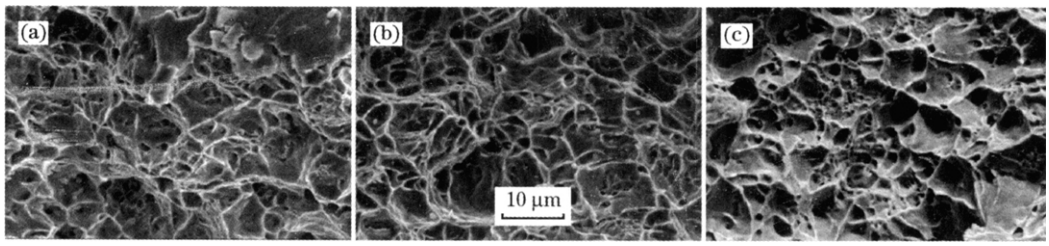

(a) D42; (b) D43; (c) D44

Fig. 13 Fracture surfaces of specimens

3 Conclusions

(1) It is found that the strength of the reinforcing steel could be substantially improved by dual phase heat treatment.

(2) The results indicated that the dual phase heat treatment could be applied to low-carbon steel with carbon content higher than 0.1% and to specimens which have sections larger than 1.0 mm. But, a fast cooling rate is the key to the process.

(3) The volume fraction and grain size of phases in the microstructure of dual phase have changed depending on austenization duration. The volume fraction of martensite has increased and the average

grain size decreased with increasing the austenization duration.

(4) The microhardnesses of the ferrite and pearlite phases in the microstructure of dual phase have changed depending on austenization duration and tempering temperature. Microhardness of the martensite phase decreases, as the microhardness of the ferrite phase increases with increasing the austenization duration. However, microhardness of both phases decreases with the increase in tempering temperature.

(5) Serrated flow behavior on the DP specimens is not observed. However, discontinuity occurs in the yield regions of the dual phase steels.

(6) The strength of the dual phase steels obtained has changed depending on microhardness and ratio of the martensite phases. It is found that the specimens which are quenched for 40 minutes of austenization duration show highest values of the yield strength, tensile strength and resilience modulus but lowest values of total elongation, reduction of the cross-sectional area and toughness.

(7) The tensile strength, yield strength and resilience modulus of the dual phase steels decrease, as the total elongation, reduction of the cross-sectional area and toughness increase.

(8) SEM fractographic studies show that cleavage fracture is observed on the fracture surfaces of dual phase induced specimens which are quenched but not tempered. Fracture features of the dual phase steels change upon to tempering heat treatment. The fracture surfaces of the specimens show that dimple fracture is the increasing dominant mechanism depending on increasing the tempering temperature.

The authors gratefully acknowledge the financial support from the Scientific Research Projects Management Council of the Firat University for this study performed under project with grant No. 2005/1119. Additionally, we would like to extend our thanks to professor Mustafa AKSOY for his valuable advice and comments.

References:

[1] Aksoy M, Esin A. Improving the Mechanical Properties of Structural Carbon Steel by Dual-Phase Heat Treatment [J]. Journal of Materials Engineering, 1988, 10(4): 281.

[2] Lankford W T. The Making, Shaping and Treating of Steel [A]. Association of Iron and Steel Engineers (AISE) 10th Edition [C]. Pittsburgh: AISE, 1985. 1264.

[3] Llewellyn D T, Hills D J. Review: Dual-Phase Steel [J]. Ironmaking and Steelmaking, 1996, 23(6): 471.

[4] Hills D J, Llewellyn D T, Evans P J. Rapid Annealing of Dual-Phase Steels [J]. Ironmaking and Steelmaking, 1998, 25(1): 47.

[5] Davies R G, Magee C L. Structure and Properties of Dual-Phase Steels [A]. Davenport T. The American Institute of Mining Metallurgical and Petroleum Engineers AIME [C]. New York: AIME, 1979. 1.

[6] Nakagawa A H, Thomas G. Microstructure-Mechanical Property Relationships of Dual-Phase Steel Wire [J]. Metallurgical Transactions, 1985, 16A(5): 831.

[7] Cribb W R, Rigsbee J M. Work-Hardening and Its Relationship to the Microstructure and Mechanical Properties of Dual-Phase Steels [A]. Kot R A, Morris J W, eds. Structure and Properties of Dual-Phase Steels [C]. New York: The American Institute of Mining Metallurgical and Petroleum Engineers AIME, 1979. 91.

[8] Speich G R. Metals Handbook [M]. 10 ed. Metals Park: ASM, 1990.

[9] Speich G R. Physical Metallurgy of Dual Phase [A]. Kot R A, Bramfitt B L. Steels in Fundamentals of Dual Phase Steels [C]. New York: The American Institute of Mining, Metallurgical, and Petroleum Engineers AIME, 1981. 1.

[10] Thomas G. Physical Metallurgy of Direct Quenched Steels [A]. Taylor K A, Thomson S W, Fletcher F B. TMS [C]. Pittsburgh: TMS, 1993. 265.

[11] Jha B K, Avtar R, Sagar D V. Structure-Property Correlation in Low Carbon Low Alloy High Strength Wire Rods/Wires Containing Retained Austenite [J]. Transactions of the Indian Institute of Metals, 1996, 49(3): 133.

[12] Park K S, Park, K T, Lee D L, et al. Effect of Heat Treatment Path on the Cold Formability of Drawn Dual-Phase Steels [J]. Materials Science and Engineering, 2007, 449A: 1135.

[13] Trejo D, Monteiro P, Thomas G, et al. Mechanical Properties and Corrosion Susceptibility of Dual-Phase Steel in Concrete [J]. Cement and Concrete Research, 1994, 24(7): 1245.

[14] Kelestemur O, Yildiz S. Effect of Various Dual-Phase Heat Treatments on the Corrosion Behavior of Reinforcing Steel Used in the Reinforced Concrete Structures [J]. Construction and Building Materials, 2009, 23: 78.

[15] ASTM E112-96, Standard Test Methods for Determining Average Grain Size (ASTM International) [S].

[16] Sarkar P P, Kumar P, Mana K M, et al. Microstructural Influence on the Electrochemical Corrosion Behaviour of Dual-Phase Steels in 3.5% NaCl Solution [J]. Materials Letters, 2005, 59: 2488.

[17] Aksoy M. An Investigation on the Improvement of Mechanical Properties of Reinforcing Steel by Dual-Phase Treatment [D]. Elazig: Firat University Institute of Science and Technology, 1985 (in Turkish).

[18] Rigsbee J M, Vanderarend P. Journal Laboratory Studies of Microstructures and Structure-Property Relationships in Dual-Phase HSLA Steels [J]. Paper Presented at TMS-AIME Fall Meeting, 1977: 56.

[19] Morrow J, Tither G. Molybdenum in Interracially Annealed Dual-Phase Steel Strip [J]. Journal Metals, 1978, 30(3): 16.

[20] Zhang C, Cai D, Liao B, et al. A Study on the Dual-Phase Treatment of Weathering Steel 09CuPCrNi [J]. Materials Letters, 2004, 58: 1524.

[21] Ahmed E, Manzoor T, Liaqat A K, et al. Effect of Microvoid Formation on the Tensile Properties of Dual-Phase Steel [J]. Journal of Materials Engineering and Performance, 2000, 9 (3): 306.

[22] Ahmed E, Priestner R. Effect of Rolling in the Intercritical Region on the Tensile Properties of Dual-Phase Steel [J]. Journal of Materials Engineering and Performance, 1998, 7 (6): 772.

[23] Sarwar M, Priestner R. Influence of Ferrite-Martensite Microstructural Morphology on Tensile Properties of Dual-Phase Steel [J]. Journal of Materials Science, 1996, 31: 2091.

[24] Erdogan M, Tekeli S, Pamuk O, et al. Surface Carburized AISI8620 Steel With Dual-Phase Core Microstructure [J]. Materials Science and Technology, 2002, 18: 840.

[25] Keleştemur O, Aksoy M, Yildiz S. Corrosion Behavior of Tempered Dual-Phase Steel Embedded in Concrete [J]. International Journal of Minerals Metallurgy and Materials, 2009, 16(1): 43.

[26] Keleştemur O. An Investigation on the Usability and Corrosion Resistance of the Dual-Phase Steel in the Reinforced Concrete Structures [D]. Elazig: Firat University Graduate School of Natural and Applied Sciences Department of Construction Education, 2008 (in Turkish).

[27] Mould P R, Skena C C. Structure and Properties of Cold-Rolled Ferrite-Martensite Steels [A]. Devanport A T. Formable HSLA and Dual-Phase Steels [C]. New York: AIME, 1977. 128.

[28] Bayram A, Uĝuz A, Ula M. Effects of Microstructure and Notches on the Mechanical Properties of Dual-Phase Steels [J]. Materials Characterization, 1999, 43(4): 259.

[29] Tamura I, Tomata Y, Akao A, et al. On the Strength and Ductility of Two Phase Iron Alloys [J]. Transactions of ISIJ, 1973, 13: 283.

[30] Davies R G. The Deformation Behaviour of a Vanadium Strengthened Dual-Phase Steel [J]. Metallurgical and Materials Transactions, 1978, A9: 41.

(Continued From Page 31)

References:

[1] JIANG Ze-yi, WANG Xia, ZHANG Xin-xin, et al. Mathematical Model of Computer Control in Tube Reheat Furnace and Its Application [J]. Acta Metallurgica Sinica, 2000, 36 (4): 429 (in Chinese).

[2] Mantyla P T, Sallinen J, Johansson L G. Novel Method to Eliminate Reheating Furnace Skidmarks [J]. AISE Steel Technology, 2002, 79(6): 31.

[3] Jang Y J, Kim S W. An Estimation of a Billet Temperature During Reheating Furnace Operation [J]. International Journal of Control, Automation, and Systems, 2007, 5(1): 43.

[4] Jaklic A, Vode F, Kolenko T. Online Simulation Model of the Slab-Reheating Process in a Pusher-Type Furnace [J]. Applied Thermal Engineering, 2007, 27(5-6): 1105.

[5] NIE Yu-hong, CHEN Hai-geng, YAO Shou-guang. Equivalent Gray Absorption Coefficient Obtained by Inverse Analysis on Non-Gray Gases System [J]. Journal of Chemical Industry and Engineering, 2005, 56(6): 1041 (in Chinese).

[6] Ahmed B, Hmaid B, Mohamed S. Non-Gray Radiation Analysis in Participating Media With the Finite Volume Method [J]. Turkish Journal of Engineering and Environmental Sciences, 2006, 30(3): 183.

[7] Byun D, Baek S W. Numerical Investigation of Combustion With Non-Gray Thermal Radiation and Soot Formation Effect in a Liquid Rocket Engine [J]. International Journal of Heat and Mass Transfer, 2007, 50(3): 412.

[8] CUI Miao, CHEN Hai-geng, XU Li, et al. Study on Emissivities and Absorptivities of Gas in Reheating Furnace [J]. Journal of Northeastern University (Natural Science), 2008, 29 (1): 97 (in Chinese).

[9] YUE Xing-wen. Application of Imaginary Planes to Heat Transfer Mathematical Models in Reheating Furnace [D]. Shenyang: Northeastern University, 1989 (in Chinese).

[10] Charette A, Larouche A, Kocaefe Y S, et al. Application of the Imaginary Planes Method to Three-Dimensional Systems [J]. International Journal of Heat and Mass Transfer, 1990, 33(12): 2671.

[11] Modest M F. Radiative Heat Transfer [M]. NewYork: McGraw-Hill Press Inc, 1993.

[12] Strohle J, Coelho P J. On the Application of the Exponential Wide Band Model to the Calculation of Radiative Heat Transfer in One- and Two-Dimensional Enclosures [J]. International Journal of Heat and Mass Transfer, 2002, 45(10): 2129.

[13] Lallemant N, Sayre A, Weber R. Evaluation of Emissivity Correlations for H_2O-CO_2-N_2/Air Mixtures and Coupling With Solution Methods of the Radiative Transfer Equation [J]. Progress in Energy and Combustion Science, 1996, 22(6): 543.

[14] CHEN Hai-geng, WANG Zi-di, WU Bin, et al. Simulation of Online Control System for Reheating Furnace [J]. Iron and Steel, 2006, 41(12): 75 (in Chinese).